Plasma Science & Technology, Vol.8, No.5, Sept. 2006

Axial Shock in a Cylindrical Plasma with Current*

HU Yemin (胡业民)[1,2], HU Xiwei(胡希伟)[3], HE Yong(何勇)[3]

[1] Department of Modern Physics, University of Science and Techonology of China, Hefei 230026, China

[2] Institute of Plasma Physics, Chinese Academy of Sciences, Hefei 230031, China

[3] College of Electrical and Electronic Engineering, Huazhong University of Science and Techonology, Wuhan 430074, China

Abstract Hugoniot relations of a two-dimensional axial shock with current and magnetic field in a cylindrical shock tube were investigated by a numerical method. The radial profiles of the magnetic field, electric current, pressures, flow velocities and temperatures between the up- and down-stream radial force-balanced plasma of the shock were revealed by numerical analysis. It is clearly found that the axial shock can lead to two effects: one is an inverse skin effect (i.e., the current density rises towards the center of the conductor), the another is a reversed current effect which occurs near the edge and about a half radius. It is also found that the radial gradient of pressure, density and temperature all become very large near the center due to the axial shock.

Keywords: axial shock, reversed current effect, inverse skin effect

PACS: *52.35.Tc*

1 Introduction

Plasma shocks have been studied widely since 1950s. In most cases, the shocks are described by a one-dimensional plane shock model. But the one-dimensional model would be invalid for the plasmas with a large electric current and self-generated magnetic fields. To our knowledge the Hugoniot relations for a two dimensional axial shock have not been investigated systematically so far. It is well known that generally for collision-dominated shocks two factors can greatly facilitate discussion of the effects of a shock wave on a fluid. First, the shock transition region may for most purposes be approximated by a discontinuity in fluid properties. Second, the macroscopic conservation equations and Maxwell equations may be integrated across the shock to give a set of equations which are independent of the shock structure and relate fluid properties on either side of the shock (namely the Hugoniot relations equations). In this paper we investigated a two-dimensional model for the axial plasma shock with a current and self-generated magnetic field. When we analyze the equilibrium in the downstream we consider the effects of the the radial distribution of the structure of the shock front. The Hugoniot relations equations are derived from the single fluid macroscopic conservation equations and Maxwell equations under the model. In this model, we try to find shock solutions where the plasma keeps equilibrium in the downstream of the shock when an equilibrium in the upstream plasma is maintained.

This paper is organized as follows. The basic equations are given in Sec. 2. The basic assumptions and reduced equations are given in Sec. 3. Then, the boundary condition and the numerical analysis are in Sec. 4. Finally, the conclusions and discussion are presented in Sec. 5.

2 Basic equations

Within the characteristic time of the variation of the up- and downstream parameters, the formation of a shock front almost does not change with time. So, we can describe the plasma shock with the static equations as follows.

Continuity equation

$$\nabla \cdot (\rho \mathbf{U}) = 0. \tag{1}$$

Momentum conservation equation

$$\nabla \cdot \mathbf{\Pi} = \mathbf{0},$$

$$\mathbf{\Pi} = \rho \mathbf{U}\mathbf{U} + \mathbf{P}\mathbf{I} + \mathbf{\Xi} - \mathbf{\Phi},$$

$$\mathbf{\Phi} = \frac{1}{4\pi}(\mathbf{B}\mathbf{B} + \mathbf{E}\mathbf{E}) - \frac{B^2 + E^2}{8\pi}\mathbf{I}, \tag{2}$$

where $\mathbf{\Xi}$ denotes the viscous stress tensor, which is a complicated function, but for a collision-dominated plasma, it may be assumed simply as follows

$$\Xi_{ij} \approx \eta(\frac{\partial u_i}{\partial x_j} + \frac{\partial u_j}{\partial x_i} - \frac{2}{3}\nabla \cdot \mathbf{u}), \ (i, j = r, \theta, z). \tag{3}$$

Energy conservation equation

$$\nabla \cdot \mathbf{S} = 0, \tag{4}$$

where

$$\mathbf{S} = \frac{\mathbf{c}}{4\pi}(\mathbf{E} \times \mathbf{B}) + \mathbf{q} + \mathbf{\Xi} \cdot \mathbf{U} + \mathbf{P}\mathbf{U} + \mathbf{U}[\rho\varepsilon + \frac{1}{2}\rho\mathbf{U}^2],$$

* supported by National Natural Science Foundation of China (No. 10175025), and in part by the JSPS-CAS Core-University Program on Plasma and Nuclear Fusion

$$\varepsilon = \frac{P}{\rho(\gamma-1)}, \quad \mathbf{q} = \kappa \bigtriangledown \mathbf{T}.$$

Maxwell equations

$$\bigtriangledown \times \mathbf{E} = 0, \quad \bigtriangledown \cdot \mathbf{B} = 0, \quad \bigtriangledown \times \mathbf{B} = \frac{4\pi}{\mathrm{c}}\mathbf{J}. \quad (5)$$

Generalized Ohm's Law:

$$\mathbf{E} + \frac{\mathbf{U}\times\mathbf{B}}{c} - \frac{m_i}{Ze\rho c}(\mathbf{J}\times\mathbf{B}) + \frac{m_i}{2Ze\rho}\bigtriangledown P - \frac{\mathbf{J}}{\sigma} = 0. \quad (6)$$

Charge conservation equation

$$\bigtriangledown \cdot \mathbf{J} = 0. \quad (7)$$

Equation of state:

$$P = R_0 \rho T, \quad R_0 \simeq \frac{(1+Z)k_B}{m_i}. \quad (8)$$

$\mathbf{J}, \mathbf{\Pi}, \mathbf{S}, \mathbf{\Phi}, \mathbf{I}$ and $\mathbf{q}$ are the current density, total momentum flow density tensor, total energy flow density, electromagnetic tensor, unit tensor and heat flow, respectively. ε, T and $\frac{1}{2}\rho u^2$ are the inner energy, plasma temperature and kinetic energy, respectively. $\mathbf{E}, \mathbf{B}$ and $\mathbf{U}$ are the electric field, magnetic field and the plasma flow velocity (which is relative to the shock front), respectively. c, m_i, e, Z, ρ, σ, κ, η, and k_B are the speed of light, ion mass, electron charge, ion charge state, plasma density, electric conductivity, thermal conductivity, coefficient of viscosity and Boltzmann's constant, respectively. Here, we take the Gassuian units.

3 Basic assumptions and reduced equations

A shock dissipation mechanism is assumed mainly to be caused by thermal conductivity, viscosity and plasma resistance. In order to reduce the equations, we assume all the physical quantities are axisymmetrical, i.e. $\partial/\partial\theta = 0$. At the shock front, we assume the relations of thermal(magnetic) pressure and plasma density as follows:

$$P = P(P_1, \rho_1, r, z) = C_p(r)\rho(r,z)^{\gamma_p},$$

$$P_B = \frac{B_\theta(r,z)^2}{8\pi} = C_B(r)\rho(r,z)^{\gamma_B}. \quad (9)$$

Generally, γ_p, γ_B should be the functions of z while, for convenience here, they are assumed to be the constants which can be "determined" by comparing the calculations obtained from the varying γ_p and γ_B with the experimental results. $C_p(r)$ and $C_B(r)$ are the functions of radial displacement only.

We put the cylindrical coordinates frame(r,θ,z) at the shock front, which moves in the axial direction with a constant velocity. In this coordinate the up-stream and down-stream plasma flow velocities are $\mathbf{U_1}$ and $\mathbf{U_2}$,respectively (in what follows, the subscript of the up- and downstream quantity are "1" and "2", respectively).

In the up-and down-stream plasma, the physical quantities meet $\partial/\partial z = 0$, and from equations $\bigtriangledown\cdot\rho\mathbf{U} = \mathbf{0}$, $\bigtriangledown\cdot\mathbf{B} = \mathbf{0}$, we can obtain $U_{r1,2} = 0$ and $B_{r1,2} = 0$. Now we assume a special case in which $U_r = 0$ and $B_r = 0$ at the shock front. So the shock front yields

$$\frac{\partial}{\partial z}(\rho U_z) = 0, \quad \frac{\partial B_z}{\partial z} = 0. \quad (10)$$

Then integrating the above two equations across the shock we obtain $\rho_2 U_{z2} = \rho_1 U_{z1} = \Gamma(r)$ and $B_{z2}(r) = B_{z1}(r)$.

For simplicity, we take $B_{z1}(r) = 0$. From Eq. (2), the poloidal momentum balance yeilds

$$\frac{\partial}{\partial z}(\rho U_z U_\theta + \frac{B_\theta B_z}{8\pi} + \Xi_{z\theta}) + \frac{\partial}{\partial r}\Xi_{r\theta} + \frac{2}{r}\Xi_{r\theta} = 0,$$

$$\Xi_{r\theta} = \eta\frac{\partial U_\theta}{\partial r} - \frac{2}{3}\eta\frac{\partial U_z}{\partial z}. \quad (11)$$

In the up-and down-stream, $\partial/\partial z = 0$, so the above equation yields

$$\frac{\partial}{\partial r}\eta\frac{\partial U_\theta}{\partial r} + \frac{2}{r}\eta\frac{\partial U_\theta}{\partial r} = 0. \quad (12)$$

It is easy to see that $U_\theta = 0$ is a solution of Eq. (12) in the up-and down-stream of the shock. So for simplicity, we take $U_{\theta 1} = U_{\theta 2} = 0$. But at the shock front, due to $\partial/\partial z \neq 0$, so perhaps $U_\theta \neq 0$ should be taken.

From Eqs. (2) and (4) and the above assumptions, we obtain

$$\frac{\partial}{\partial r}(P + \frac{B_\theta^2}{8\pi}) + \frac{B_\theta^2}{4\pi r} - \frac{\rho U_\theta^2}{r} + (\bigtriangledown\cdot\Xi)_r - \frac{E_r}{4\pi}\bigtriangledown\cdot E = 0, \quad (13)$$

$$\frac{\partial}{\partial z}(\Gamma U_z + P + \frac{B_\theta^2}{8\pi}) + (\bigtriangledown\cdot\Xi)_z - \frac{E_z}{4\pi}\bigtriangledown\cdot E = 0, \quad (14)$$

$$\frac{\partial}{\partial z}(\frac{\gamma_p}{\gamma_p - 1}PU_z + q_z + \Xi_{zz}U_z + \Xi_{z\theta}U_\theta + \frac{\Gamma}{2}U_z^2 + \frac{c}{4\pi}E_r B_\theta)$$

$$+\frac{1}{r}\frac{\partial}{\partial r}r(q_r + \Xi_{rz}U_z + \Xi_{r\theta}U_\theta) - \frac{c}{4\pi r}\frac{\partial}{\partial r}(rE_z B_\theta) = 0, \quad (15)$$

$$E_\theta = 0, \quad \frac{\partial E_r}{\partial z} = \frac{\partial E_z}{\partial r}, \quad (16)$$

$$E_r = \frac{U_z B_\theta}{\mathrm{c}} - \frac{m_i}{e\rho c}j_z B_\theta - \frac{m_i}{2Ze\rho}\frac{\partial P}{\partial r} + \frac{j_r}{\sigma},$$

$$E_z = \frac{m_i}{e\rho c}j_r B_\theta - \frac{m_i}{2Ze\rho}\frac{\partial P}{\partial z} + \frac{j_z}{\sigma}.$$

$$j_r = -\frac{c}{4\pi}\frac{\partial B_\theta}{\partial z}, \quad j_\theta = 0, \quad j_z = \frac{\mathrm{c}}{4\pi r}\frac{\partial}{\partial r}(rB_\theta). \quad (17)$$

In the upstream and downstream, $U_r = 0$, $U_\theta = 0$, $\partial U_z/\partial z = 0$, $\partial U_z/\partial\theta = 0$, from (3), one yields

$$(\bigtriangledown\cdot\Xi)_r = 0, \quad \Xi_{z\theta} = \Xi_{r\theta} = 0. \quad (18)$$

At the shock front, $U_r = 0$, $U_\theta \neq 0$, $\partial U_z/\partial z \neq 0$, $\partial U_z/\partial\theta = 0$, from (3), one yields

$$(\nabla \cdot \Xi)_z = \frac{1}{r}\frac{\partial}{\partial r}(r\Xi_{rz}) + \frac{\partial}{\partial z}\Xi_{zz}$$
$$= \frac{1}{r}\frac{\partial}{\partial r}(r\eta\frac{\partial U_z}{\partial r}) + \frac{\partial}{\partial z}(\frac{\eta}{3}\frac{\partial U_z}{\partial z}). \quad (19)$$

In addition, in a quasi-neutral plasma, as compared with the magnetic field, the electric field stress can be ignored in Eqs. (13) and (14). So substituting (18) into (13) and (19) into (14), then the radial balance equations in the up- and down-stream and an axial balance equations at the shock front can be given,

$$\frac{\partial}{\partial r}(P_1 + \frac{B_{1\theta}^2}{8\pi}) + \frac{B_{1\theta}^2}{4\pi r} = 0, \quad (20)$$

$$\frac{\partial}{\partial r}(P_2 + \frac{B_{2\theta}^2}{8\pi}) + \frac{B_{2\theta}^2}{4\pi r} = 0. \quad (21)$$

$$\frac{\partial}{\partial z}(\Gamma U_z + P + \frac{B_\theta^2}{8\pi} + \frac{\eta}{3}\frac{\partial U_z}{\partial z}) + \frac{1}{r}\frac{\partial}{\partial r}(r\eta\frac{\partial U_z}{\partial r}) = 0, \quad (22)$$

To calculate the integral of the two sides of Eqs. (22), (15) and (16) across the up-(z_1) and down-stream(z_2) and use the conditions for meeting up- and down-stream $\partial/\partial z = 0$, we can obtain

$$[\Gamma U_z + P + \frac{B_\theta^2}{8\pi}]_1^2 = \frac{1}{r}\frac{\partial}{\partial r}(r\Re_1), \quad (23)$$

$$[\frac{\gamma_p}{\gamma_p - 1}PU_z + \frac{\Gamma}{2}U_z^2 + \frac{c}{4\pi}E_rB_\theta]_1^2 = \frac{1}{r}\frac{\partial}{\partial r}(r\Re_2), \quad (24)$$

$$[\frac{U_zB_\theta}{c} - \frac{m_i}{e\rho c}j_zB_\theta - \frac{m_i}{2e\rho}\frac{\partial P}{\partial r}]_1^2$$
$$= \frac{\partial}{\partial r}\int_{z_1}^{z_2}(\frac{m_i}{Ze\rho c}j_rB_\theta - \frac{m_i}{2Ze\rho}\frac{\partial P}{\partial z})\mathrm{d}z + \frac{\partial}{\partial r}\Re_3. \quad (25)$$

$$\Re_1 = -\int_{z_1}^{z_2}\eta\frac{\partial U_z}{\partial r}\mathrm{d}z,$$

$$\Re_2 = -\int_{z_1}^{z_2}(q_r + \Xi_{rz}U_z + \Xi_{r\theta}U_\theta - \frac{c}{4\pi}E_zB_\theta)\mathrm{d}z,$$

$$\Re_3 = \int_{z_1}^{z_2}\frac{j_z}{\sigma}\mathrm{d}z.$$

Here Eqs. (20)(21) and (23)~(25) are defined as the Rankine-Hugoniot equations of two dimensions shock with a magnetic, current and electric field. Using (9), the first terms on the right hand side of Eq. (25) can be integrated explicitly. $\Re_1, \Re_2$ and $\Re_3$ cannot be integrated explicitly and they are all unknown. $\Re_1$ denotes the effect of the viscosity on the radial momentum flow, $\Re_2$ denotes the effects of the radial heat flow, work of the radial viscosity force and the radial electromagnetic energy on the total radial energy flow, and $\Re_3$ denotes the effect of the finite electric conductivity on the axial electric field. The viscosity, thermal conductivity and finite electric conductivity all vary independently across the shock. So $\Re_1, \Re_2$ and $\Re_3$ are all considered as independent variables. Thus the set of Eqs. (8)(9)(10)(17)(20)~(25) has eleven equations for nineteen variables $\rho_{1,2}, U_{z_{1,2}}, P_{1,2}, T_{1,2}, B_{\theta_{1,2}}, j_{r_{1,2}}, j_{z_{1,2}}, C_p, C_B, \Re_1, \Re_2$ and $\Re_3$. If the radial profiles of B_{θ_1}, U_{z_1} and T_1 are given, then we can eliminate some of the variables as $\rho_{1,2}, U_{z_1}, T_{1,2}, B_{\theta_1}, j_{r_{1,2}}, j_{z_{1,2}}, C_p$ and C_B, by using (8) (9)(10) and (17). Thus we can reduce the set of equations to (20) ~ (25) only for variables $P_{1,2}, B_{\theta_2}, U_{z_2}, \Re_1, \Re_2$ and $\Re_3$. For simplicity, we would set $\Re_1 = \Re_{1c}$, $\Re_3 = \Re_{3c}$($\Re_{1c}$ and $\Re_{3c}$ are constants) and retain only $\Re_2$ as a variable to close this set of equations.

Let

$$\alpha = P_2/P_1, \quad \beta = U_{z2}/U_{z1}, \quad b = B_{2\theta}/B_{1\theta},$$
$$\xi = r/r_0, \quad \chi = P_1/P_0, \quad (26)$$

where P_0 and r_0 are the reference pressure and the radius of Z-pinch, respectively. Using (9) and (26), the Eqs. (20)~(25) yield the dimensionless equations as follows:

$$\frac{\partial}{\partial\xi}(\chi + Q_0) = -2\frac{Q_0}{\xi}, \quad (27)$$

$$\frac{\partial}{\partial\xi}(\alpha\chi + Q_0b^2) = -2\frac{b^2Q_0}{\xi}, \quad (28)$$

$$\gamma_pM^2(\beta - 1) + \alpha - 1 + Q(b^2 - 1) - \frac{1}{\xi\chi}\frac{\partial}{\partial\xi}(\xi f_v) = 0, \quad (29)$$

$$\frac{\gamma_p}{2}M^2(\beta^2 - 1) + \frac{\gamma_p}{\gamma_p - 1}(\alpha\beta - 1) + 2bQf_E$$
$$+2QE_1(b - 1) + \frac{1}{u\chi\xi}\frac{\partial}{\partial\xi}(\xi f_T) = 0. \quad (30)$$

$$2\vartheta_B\frac{\partial}{\partial\xi}[uQt(\beta b^2 - 1)] + \vartheta_p\frac{\partial}{\partial\xi}[ut(\alpha\beta - 1)] = uBf_E. \quad (31)$$

Here,

$$M = \frac{U_{z1}}{c_s}, \quad c_s = (\frac{\gamma_pP_1}{\rho_1})^{1/2}, \quad Q_0 = \frac{B_{1\theta}^2}{8\pi P_0}, \quad Q = \frac{Q_0}{\chi},$$
$$P_0 = \frac{B_{00}^2}{8\pi}, \quad B_{00} = \frac{2I_{00}}{r_0c}, \quad t = \frac{T_1}{T_0}, \quad \vartheta = \frac{I_0}{I_{00}} = \frac{B_0}{B_{00}},$$
$$f_v = C_v\xi(1 - \xi), \quad C_v = \frac{\Re_{1c}}{P_0}, \quad f_T = -\frac{\Re_2}{r_0P_0U_{z0}},$$
$$f_E = \beta b - 1 - \frac{w}{2}E_{21} - \frac{w}{8}P_{21},$$
$$E_{21} = \frac{\beta b^2B^2}{\xi} + (\beta b^2 - 1)B\frac{\partial B}{\partial\xi} - \frac{B^2}{\xi} + \beta bB^2\frac{\partial b}{\partial\xi},$$
$$P_{21} = (\alpha\beta - 1)\frac{\partial\chi}{\partial\xi} + \beta\chi\frac{\partial\alpha}{\partial\xi},$$
$$E_1 = 1 - (B\frac{\partial B}{\partial\xi} + \frac{B^2}{\xi})\frac{w}{2} - \frac{w}{8\theta^2}\frac{\partial\chi}{\partial\xi},$$

$$w=\frac{\vartheta t}{uB\chi},\ B=\frac{B_{\theta 1}}{B_0},\ u=\frac{U_{z1}}{U_{z0}},\ j_{00}=\frac{I_{00}}{\pi r_0^2},$$

$$U_{z0}=\frac{j_{00}}{Zen_0},\ \vartheta_B=-\frac{1}{8\vartheta}\frac{\gamma_B}{\gamma_B-1},\ \vartheta_p=-\frac{1}{8\vartheta}\frac{\gamma_p}{\gamma_p-1},$$

where M, c_s, B_{00}, I_{00}, n_0, I_0 and B_0 are the upstream Mach number, ion acoustic velocity, reference magnetic field, reference current, reference plasma number density, axial plasma current and poloidal magnetic field at the plasma boundary ($r=r_0$), respectively. q_r is a radial component of the heat flow. In addition, q_r is a unclear function at the shock front, so f_T is taken as a unknown variable.

4 Boundary condition and numerical analysis

Using Eq. (7), it can be deduced that the total current passing through the shock front is unchanged, thus the poloidal magnetic at both edges of the upstream and downstream of the shock is not changed. Therefore we can obtain

$$b|_{\xi=1}=1. \tag{32}$$

Using (32) one can obtain from Eqs. (29) and (30)

$$\alpha|_{\xi=1}=1+\frac{\gamma_p(M_1^2-1)-F_v}{\gamma_p+1}+\frac{\gamma_p\sqrt{(M_1^2-1)^2+F}}{\gamma_p+1}, \tag{33}$$

$$\beta|_{\xi=1}=\frac{\gamma_pM_1^2+1-F_v}{(\gamma_p+1)M_1^2}-\frac{\sqrt{(M_1^2-1)^2+F}}{(\gamma_p+1)M_1^2}, \tag{34}$$

where

$$F=2\gamma_pM_1^2(\frac{\gamma_p^2-1}{\gamma_p^2}F_e-F_v)+(F_v-1)^2-1,$$

$$M_1=M|_{\xi=1},\ F_e=[2Qf_E+(u\chi\xi)^{-1}\frac{\partial(\xi f_T)}{\partial\xi}]|_{\xi=1},$$

$$F_v=\frac{1}{\xi\chi}\frac{\partial}{\partial\xi}(\xi f_v)|_{\xi=1}.$$

F_e is a complicated function and is considered as the effects of the magnetic field, current and heat flow. F_v is an effect of the radial velocity gradient (hence viscosity) at the boundary across the shock. They can also be determined by comparing the calculated results with different F_e and F_v's to the experimental data. Because α and β are both real quantities, from (33) and (34), we have $(M_1^2-1)^2+F\geq 0$, i.e. $F\geq F_c=-(M_1^2-1)^2$.

So we can obtain

$$F_e\geq F_{ec}=\frac{\gamma_p^2}{\gamma_p^2-1}[F_v-\frac{(M_1^2-1)^2+(F_v-1)^2-1}{2\gamma_pM_1^2}]. \tag{35}$$

When $F_e=F_v=0$, (33) and (34) will reduce to a general plasma case without a magnetic, electric current, heat flow or radial velocity gradient. Generally F is a negative value and for simplicity we will set the value of F from $F_c\sim 0$.

Considering no energy exchange between the system of the cylindrical plasma and the external environment, we can assume $\Re_2|_{\xi=1}=0$, i.e.

$$f_T|_{\xi=1}=\frac{\Re_2|_{\xi=1}}{P_0u_{z0}}=0. \tag{36}$$

The radial distribution of the magnetic field, flow velocity and plasma temperature in the upstream can be set as:

$$B_{1\theta}=B_0\frac{2\xi}{1+\xi^2},$$

$$U_{z_1}=M_0C_{s0}[u_0+u_c(1-\xi^2)^2],$$

$$T_1=T_0[T_b+T_c(1-\xi^2)^2], \tag{37}$$

where $C_{s0}=\sqrt{\gamma_pk_BT_0/m_i}$, $k_B=1.602\times10^{-12}$erg/eV. M_0, u_0 and T_b are the given constants. We take $I_{00}=1.0\times10^{15}statampere=333.3\,\mathrm{kA}$, $T_0=1000\,\mathrm{eV}$, $r_0=5\,\mathrm{cm}$.

Then, solving Eqs. (27)~(31) with the above conditions, we can obtain the radial profiles of α,β,b,χ and f_T. In what follows, if without special claims, all the abscissas and vertical coordinates of the figures are the normalized radius ξ and the pure dimensionless number respectively and also all the values of the parameters and the upstream boundary pressure are taken as follows:

$$I_0=32\,\mathrm{kA}, M_0=1.6,\ Z=1,\ \gamma_p=1.72,\ \gamma_B=3.0,$$

$$\Re_{1c}=0,\ \Re_{3c}=0,\ T_b=0.12,\ T_c=0.4, u_0=0.8,$$

$$u_c=0.12,\ F_e=F_{ec}+0.172,\ \chi_0=\chi|_{\xi=1}=0.005. \tag{38}$$

In the up-stream, when the profiles of the poloidal magnetic and the plasma temperature are given such as that in (37), we can obtain the profiles of the pressure P_1 and plasma number density n_1 ($=n_i+n_e$) by using equations (8) and (20). Fig. $1(a_1)\sim(a_2)$ show the radial profiles of the up-stream pressure plasma number density change with axial current. Fig. $2(b_1)\sim(b_2)$ show the radial profiles of the up-stream pressure and plasma number density change with boundary pressure values. It is found that the axial current and the boundary pressure value have a notable effect on the profiles of the pressure and plasma density in a cylindrical equilibrium plasma.

a. The radial distributions of the down-stream quantities with the given radial profiles of the current density, flow velocity and plasma temperature in the up-stream

We have given the radial profiles of the current density, flow velocity and plasma temperature in the up-stream as (37). Fig. $3(a)\sim(c)$ show the radial profiles

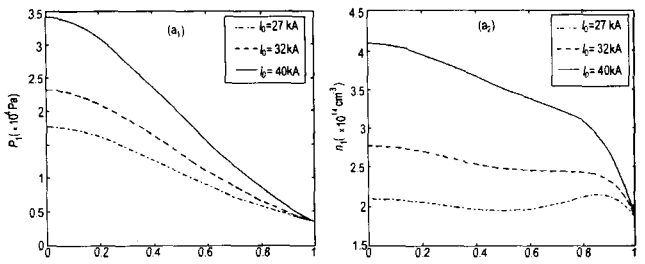

Fig.1 Radial profiles of the pressure (a_1) and plasma number density (a_2) in the up-stream equilibrium plasma vary with different axial current

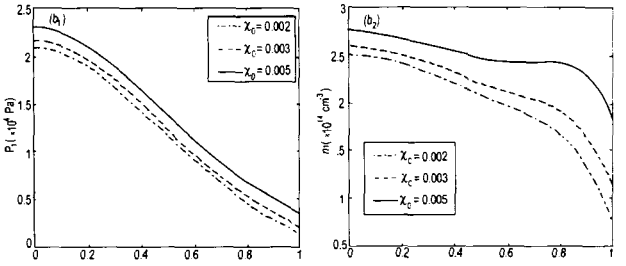

Fig.2 Radial profiles of the pressure (a_1) and plasma number density (a_2) in the up-stream equilibrium plasma vary with different boundary pressure values

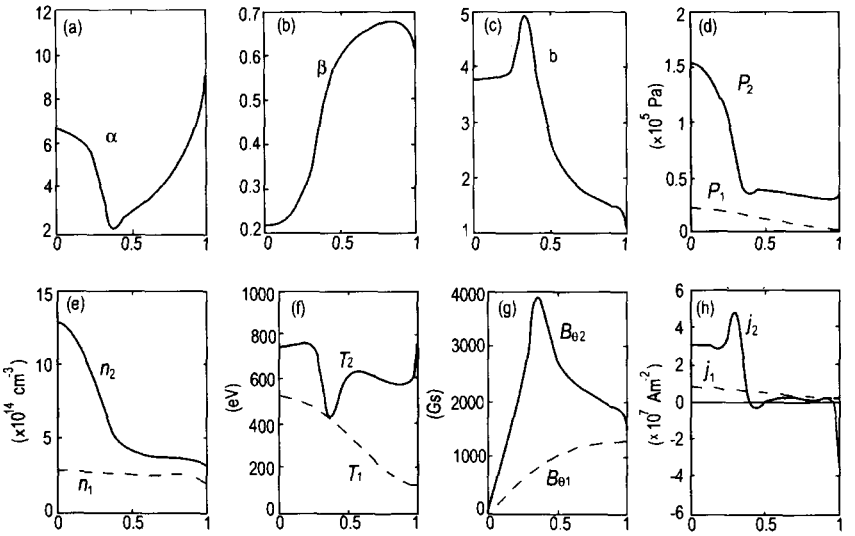

Fig.3 Radial profiles of the ratio of (a) the down-stream pressure to up-stream pressure and (b) the down-stream flow velocity to up-stream flow velocity and the comparison of the radial profiles of the (c) flow velocity, (d) pressure, (e) number density and (f) temperature of the up-stream plasma with those of the down-stream plasma, respectively

of the ratio of the down-stream pressure, velocity and poloidal magnetic field to the corresponding quantities, respectively. It is found that the weakest shock is located near $\xi \approx 0.4 \sim 0.5$ where the current density and magnetic fields are largest. Fig. $3(d) \sim (h)$ show the comparison between the profiles of the pressure, number density, temperature, poloidal magnetic and axial current density of the up-stream plasma and those of the down-stream plasma. Figs. $3(d) \sim (f)$ clearly show that the axial shock can also be enhanced to a pinch plasma, which is just similar to the radial shock, especially near the core of the down-stream plasma. The gradient of pressure, density and temperature all become very large, which is similar to the internal transport barrier in a tokamak and which can be explained qualitatively by what is in the down stream. The maximum poloidal magnetic field (see Fig. $3(g)$) is near the core plasma. Furthermare the cone plasma pinch gets enhanced at the place where the magnetic well gets deeper than that in the upstream. From Figs. $3(f) \sim (g)$, we can also find that the lowest temperature is located at $\xi \simeq 0.3 \sim 0.4$ where just the maximum of the poloidal magnetic field and axial current density are located, and this means that at the shock front some thermal energy may be converted into the magnetic energy.

Fig. $3(g)$ and (h) show the radial profiles of the poloidal magnetic field and axial current density in the up- and down-stream of the shock, respectively. It can be clearly seen that in the down-stream maximum crest current density can be made by the shock to be away from the center and some also to be reversed at the middle ($\xi \simeq 0.4 \sim 0.6$) and the edge (Fig. $3(h)$), which may be explained qualitatively by the radial current (j_r) that would occur at the shock front and its varied radial distribution may further affect the radial profiles of the axial current density. We can also find that here the profiles of the poloidal magnetic field and axial current density in the down-stream (shown in Fig. $3(g)$ and (h)) are in rough agreement with those from the experiment [1] at the time $t = 1.8\mu s$ (when $I_0 = 31.9$ kA). So we believe the axial shock may be a mechanism to cause the current reversal.

b. Effects of C_v and F_e.

Fig. $4(a)$ shows the effects of the varied C_v and F_e on the radial profiles of the current density in the down-stream. Here, the $C_v(= \Re_{1c}/P_0)$ represents the effects of the viscosity across the shock. It is found that the central current density increases sharply with increase of C_v if $C_v > 0$ and also decreases sharply with the de-

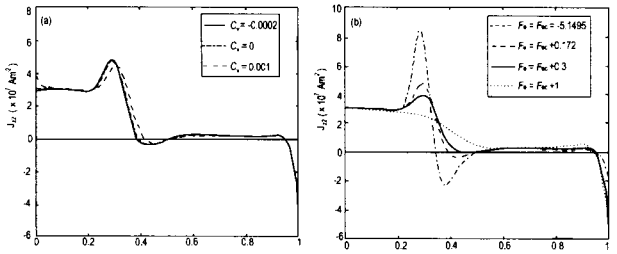

Fig.4 Radial profiles of the current density in the down-stream change with different C_v's and F_e's

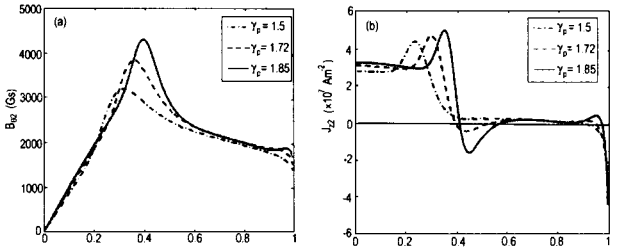

Fig.5 Profiles of axial current density and poloidal magnetic change with different γ_p's in the down-stream

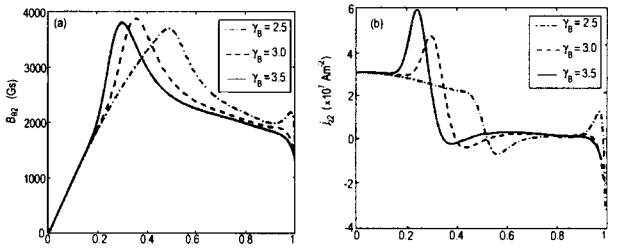

Fig.6 Profiles of axial current density and poloidal magnetic change with different γ_B's in the down-stream

crease of C_v if $C_v < 0$. According to the experiments where the central current density is always limited, we can conclude that C_v should be very small and so we take $C_v \simeq 0$. F_e is considered as the effects of the magnetic field, current and heat flow at the boundary across the shock. From (35) and (38), we can obtain $F_{ec} = -5.1495$. Fig. 4(b) shows that the maximum current density decrease with the decrease of the absolute value of F_e. Comparing the results of the pilot calculations with those of the experiments, we take $F_e = F_{ec} + 0.172 = -4.9775$ as a proper value.

c. Effects of γ_p and γ_B.

At the shock front, the relations of the plasma density to the thermal and magnetic pressure are not clear, so we have only assumed the relations to be those in Eq. (9). Figs. (5) and (6) show the radial profiles of the poloidal magnetic field and axial current density vary with different γ_p and γ_B,respectively. We find when $\gamma_p \approx 1.4 \sim 2.0$, and $\gamma_B \approx 2.5 \sim 4.0$ the radial profiles of the poloidal magnetic field and axial current in the downstream are in rough agreement with the results of experiments [1] provided that the necessary conditions are given, such as (37) and (38). We can find here that γ_p is close to the specific heat ratio $\gamma = 5/3$ for a monatomic gas and this means that shock compression is close to the adiabatic compression, while γ_B is much larger than the equivalent magnetic adiabatic index

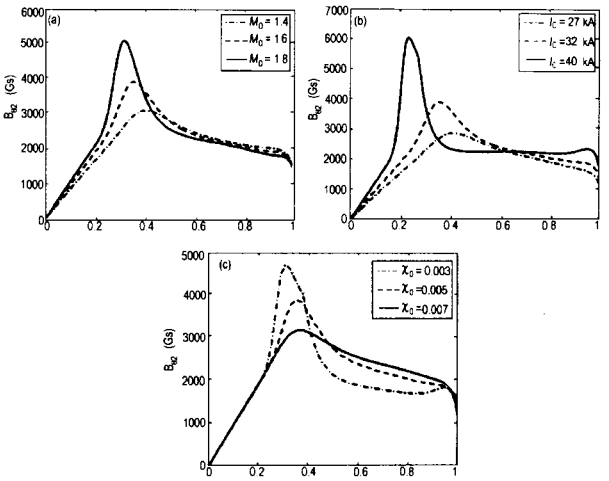

Fig.7 Radial profiles of the poloidal magnetic field in the down-stream change with different M_0, I_0 and χ_0's

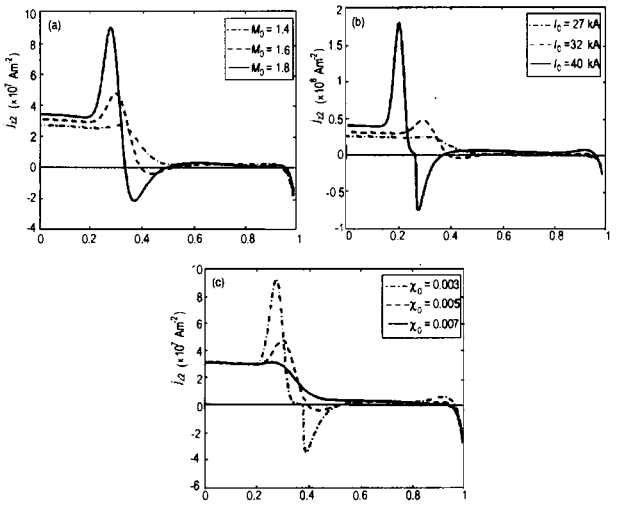

Fig.8 Radial profiles of the axial current density in the down-stream change with different M_0, I_0 and χ_0's

γ_m which equals to 4/3 for the compression of an ideal magnetofluid.

d. Effects of M_0, total axial current I_0 and up-stream pressure boundary value χ_0.

The different M_0 represents the change of the magnitude of the flow velocity. Figs. 7(a)~(c) and Figs. 8(a)~(c) show the radial profiles of the poloidal magnetic field and axial current density in the down-stream with different M_0, I_0 and χ_0. It is found that the maximum magnetic field and current density are both away from the axis and also their corresponding maximum magnitude decreases with the decrease of M_0 and I_0 but the increase of χ_0 reciprocally.

Figs. $10(a) \sim$ (c) and Figs. $9(a) \sim$ (c) show the radial profiles of the shock strength, i.e. the ratio of down-stream pressure to up-stream pressure, and thermal pressure in the down-stream change with different M_0, I_0 and χ_0. From Fig. 10(a)and Fig. 9(a), we find that the pressure and shock strength increase grossly with the increase of M_0 and reciprocal with the reversed current occurring. From Fig. 9(b) and Fig. 8(b), we can

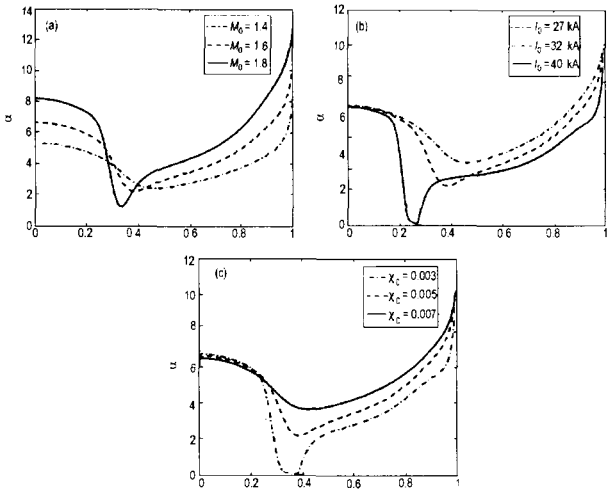

Fig.9 Radial profiles of the shock strength change with different M_0, I_0 and χ_0's

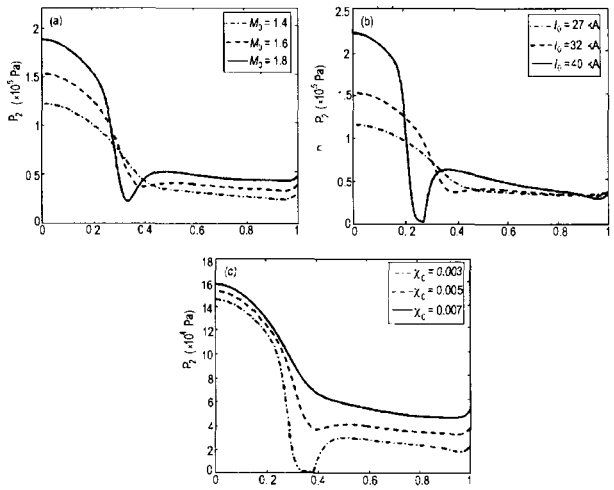

Fig.10 Radial profiles of the pressure in the down-stream change with different M_0, I_0 and χ_0's

also find that the shock strength decreases grossly with the increase of I_0 (hence the electric current density), which is in agreement with the results of Ref. [3]. From Figs. 8(a) $\sim$ (c) and Figs. 9(a) $\sim$ (c), it is evident that the minimum shock strength is just located near the place where the magnitude of the magnetic field is maximum and the current density is minimum.

5 Conclusions and discussion

In conclusion, numerical analysis of the Hugoniot relations of a two-dimensional shock has been conducted. It is clearly shown that the reversed current profiles will be formed in the downstream plasma under certain conditions. Our investigations also show that the axial shock will also result in that the gradient of pressure, density and temperature all become very large near the center, which is similar to ITB(inner transport barriers) in tokamak plasmas.

When the plasmas are in a compressional phase an axial non-uniform stress may cause an axial flow(or a puff), and the shock will be built if the flow (puff) velocity is large enough. Similar to the case of neutral beam injection (NBI) or radio frequency (RF) to heating in tokamak, if the plasma flow driven by NBI or radio-frequency field [2] is large enough, the toroidal shock may also occur. As is known, there is a strong connection between the plasma rotation (flow), the transition from L to H mode and the formation of transport barriers in tokamak plasmas [4,5]. When the plasma flow velocity is large enough, a shock will be built, then there may also be a connection between the shock and the L-H mode transition. The connection between the poloidal shock [6], the transition from L to H mode and the formation of transport barriers in tokamak plasmas has been investigated, but the connection between the toroidal shock and the plasms confinement has rarely been reported. So this work may also be an enlightenment as to further propose an axial shock model which is correlated to the L- to H-mode transition in tokamak plasmas. We are collecting evidence for the toroidal shock mode correlating to the L- to H-mode transition in tokamak plasmas and will carry on our work further.

Acknowledgements

This work was done partially during HU Yemin's visit at NIFS. He wishes to thank Prof. SANUKI H. for his hospitality and helpful discussion about this work.

References

1 Haines M G. 1959, Proc. Phys. Soc., London, 74: 576
2 Jones I R, Silavawiananai C. 1980, Plasma Phys., 22: 501
3 Lee Ki-Tae, Kim Dong-Eon, Kim Seong-Ho. 2000, Phys. Rev. Lett., 85: 3834
4 Ikezi H, Mima K, Nishikawa Kyoji, et al. 1976, Phys. Rev. Lett., 36: 794
5 HU Yemin, HU Xiwei. 2003, Phys. Plasmas, 10: 2704
6 Shaing K C, Crume E C, Jr, et al. 1989, Phys. Rev. Lett., 63: 2369
7 Rice J E, Boivin R L, Bonoli P T, et al. 2001, Nuclear Fusion, 41: 277
8 Shaing K C, Hazeltine H D, Sanuki H. 1992, Phys. Fluids B, 4: 404

(Manuscript received 10 August 2005)
E-mail address of HU Yemin: yeminhu@ipp.ac.cn